SLAC–PUB–5977
October 1992
E

NEW MEASUREMENTS OF THE τ LEPTON MASS*

HELMUT MARSISKE

Stanford Linear Accelerator Center
Stanford University, Stanford, California 94309

ABSTRACT

We report on recent measurements of the mass of the τ lepton, performed by the ARGUS, BES and CLEO experiments. The presentation follows closely References 1, 2 and 3.

Invited talk at the
SECOND WORKSHOP ON TAU LEPTON PHYSICS
The Ohio State University
Columbus, Ohio, USA
September 8-11, 1992

* Work supported in part by the Department of Energy, contract DE–AC03–76SF00515.

NEW MEASUREMENTS OF THE τ LEPTON MASS[†]

HELMUT MARSISKE

Stanford Linear Accelerator Center
Stanford University, Stanford, California 94309, USA

ABSTRACT

We report on recent measurements of the mass of the τ lepton, performed by the ARGUS, BES and CLEO experiments. The presentation follows closely References 1, 2 and 3.

1. Introduction

In the Standard Model the τ is a third generation sequential lepton having the same type of electro-weak interactions as the electron and muon, including the same universal coupling constant; this is the concept of lepton universality. Within the Standard Model, leptonic decays of the muon and tau can be calculated including radiative corrections![4]

$$\Gamma(L \to \nu_L l \nu_l(\gamma)) = \hbar \frac{B(L \to \nu_L l \nu_l(\gamma))}{\tau_L} \tag{1.1}$$
$$= \frac{G_F^2(L) m_L^5}{192\pi^3} \left[f\left(\frac{m_l^2}{m_L^2}\right) \right] \left[1 + \frac{3}{5}\frac{m_L^2}{m_W^2} \right] \left[1 + \frac{\alpha(m_L)}{2\pi} \left(\frac{25}{4} - \pi^2 \right) \right] ,$$

where the first term in brackets is a phase space correction, $f(x) = 1 - 8x + 8x^3 - x^4 - 12x^2 \ln x$, the second term corrects for the non-local W propagator, and the third term represents the radiative corrections with $\alpha^{-1}(m_\mu) = 136$ and $\alpha^{-1}(m_\tau) = 133.3$. Note that the decay width depends on the mass of the parent lepton raised to the fifth power.

† Work supported in part by the Department of Energy, contract DE-AC03-76SF00515.

Equation (1.1) is used to extract the coupling constant, G_F, from measured muon quantities,[5] *i.e.*, the muon lifetime, electronic branching fraction and muon mass, yielding

$$G_F(\mu) = (1.16639 \pm 0.00001) \times 10^{-5}\,\mathrm{GeV}^{-2}\ . \tag{1.2}$$

If, however, the corresponding measured τ quantities[5] are used, one gets

$$G_F(\tau) = (1.13784 \pm 0.00968) \times 10^{-5}\,\mathrm{GeV}^{-2}\ . \tag{1.3}$$

Thus,

$$\frac{G_F^2(\tau)}{G_F^2(\mu)} = 0.941 \pm 0.019 \pm 0.014 \pm 0.010\ , \tag{1.4}$$

where the error contributions from the lifetime, the electronic branching fraction and the mass are listed separately. This represents a 2.4 standard deviation disagreement with lepton universality, which implies a value of unity for this ratio, and is often referred to as the consistency problem. Note that the error in Equation (1.4) is completely dominated by the τ measurements. We will focus here on new much more precise τ mass measurements; much improved lifetime and branching fraction measurements are presented elsewhere in these proceedings.

Until recently, the only method applied in determining the τ mass is based on a measurement of the $\tau^+\tau^-$ production cross section in the threshold region. There existed only four measurements yielding an average value of $m_\tau = 1784.1^{+2.7}_{-3.6}\,\mathrm{MeV}$.[5] The average was completely dominated by the result from the DELCO experiment,[6] $m_\tau = 1782^{+2}_{-7}\,\mathrm{MeV}$, which was later refined to $m_\tau = 1783^{+3}_{-4}\,\mathrm{MeV}$. The precision of this method can be greatly improved by applying an optimized scan strategy in a very narrow center-of-mass energy range ($\sim 25\,\mathrm{MeV}$) around threshold and by selecting a virtually background free final state. The BES experiment recently chose to perform such a measurement.

This measurement technique is not available to the ARGUS and CLEO experiments, which operate at center-of-mass energies around 10 GeV — far above τ pair production threshold. Thus, both experiments have developed novel methods that instead exploit the kinematics in hadronic τ decay.

2. The BES τ Mass Measurement

A measurement of the $\tau^+\tau^-$ production cross section in the region most sensitive to the τ mass — a few MeV around threshold — provides the opportunity to measure the τ mass with greatly improved precision. We present such a measurement[2] using the Beijing Spectrometer (BES) at the Beijing Electron Positron Collider (BEPC). The $\tau^+\tau^-$ events are identified by means of the $e-\mu$ topology, which provides the best combination of high detection efficiency and low background; the mass value is obtained from a fit to the energy dependence of the cross section. The measurement is independent of the ν_τ mass.

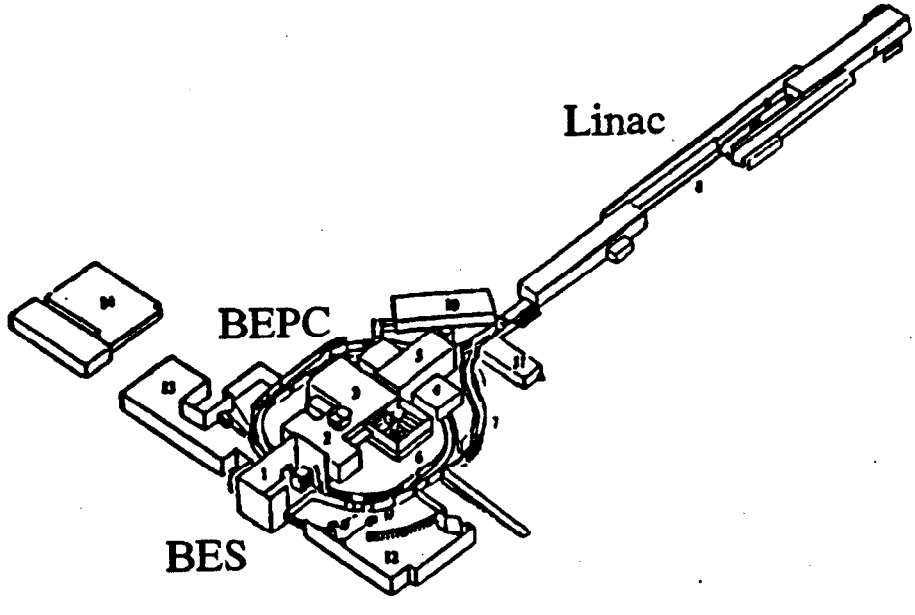

Figure 1. The Beijing Electron Positron Collider.

The BEPC[7] operates in the 3 to 5 GeV center-of-mass energy range. Near $\tau^+\tau^-$ threshold, the peak luminosity is $5 \times 10^{30}\,\mathrm{cm}^{-2}\mathrm{s}^{-1}$, the luminosity-weighted uncertainty in the mean center-of-mass energy is 0.10 MeV, and the spread in the center-of-mass energy of the collider is about 1.4 MeV. The absolute energy scale and energy spread are determined by interpolation between the results of repeated scans of the J/ψ and ψ' resonances.

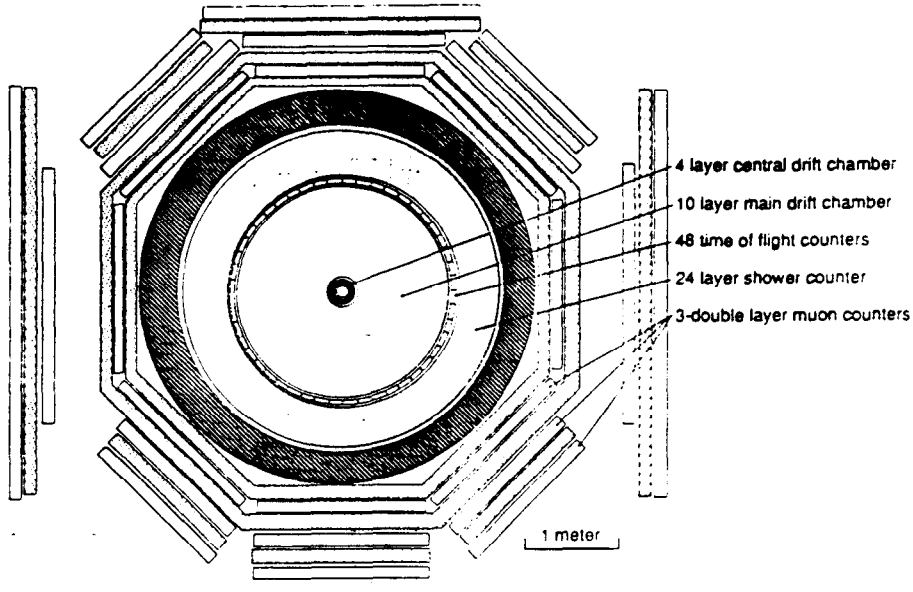

Figure 2. Axial view of the Beijing Spectrometer.

The BES is a solenoidal detector[7] with a 0.4 T magnetic field. Charged track reconstruction is performed by means of a cylindrical drift chamber which provides solid angle coverage of 85% of 4π. The momentum resolution is $\sigma_p/p = 0.021\sqrt{1+p^2}$ (p in GeV). Measurements of dE/dx with resolution 8.5% allow particle identification. An inner drift chamber is used for trigger purposes. Scintillation counters measure the time-of-flight of charged particles over 76% of 4π with a Bhabha resolution of 330 ps. A cylindrical twelve-radiation-length Pb/gas electromagnetic calorimeter operating in limited streamer mode covering 80% of 4π achieves energy resolution $\sigma_E/E = 0.25/\sqrt{E(\mathrm{GeV})}$, and spatial resolution

$\sigma_\phi = 4.5\,\text{mrad}$, $\sigma_z = 2\,\text{cm}$. End-cap time-of-flight counters and shower counters are not used in this analysis. Finally, a three-layer iron flux return instrumented for muon identification yields spatial resolutions $\sigma_z = 5\,\text{cm}$, $\sigma_{r\phi} = 3\,\text{cm}$ over 68% of 4π for muons with momentum greater than 550 MeV.

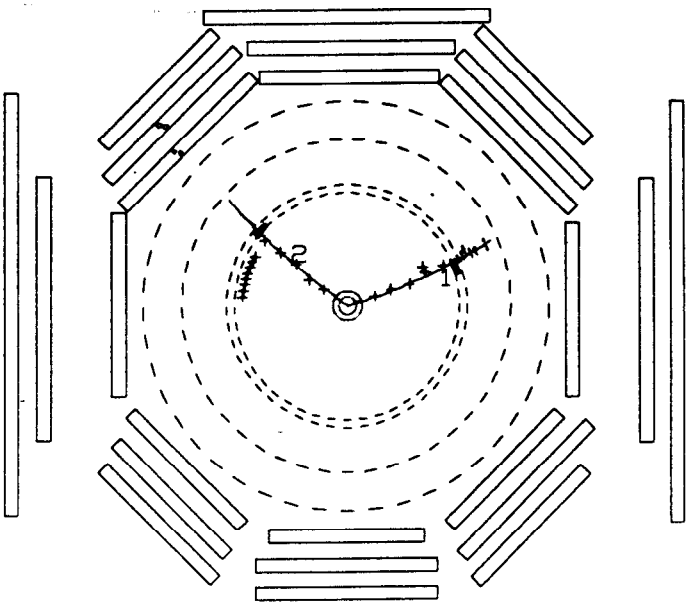

Figure 3. Axial view of a selected $e - \mu$ event in the BES detector.

In the data analysis, the event selection for $e - \mu$ candidates requires : (1) exactly two oppositely-charged tracks having momentum between 350 MeV and the maximum for an electron from τ decay, (2) each track's point of closest approach to the intersection point to satisfy $|x| < 1.5\,\text{cm}$, $|y| < 1.5\,\text{cm}$ and $|z| < 15\,\text{cm}$, (3) $2.5° < \theta_{\text{acol}}{}^{\star} < 177.5°$, $\theta_{\text{acop}} > 10°$, and $(\theta_{\text{acol}} + \theta_{\text{acop}}) > 50°$, (4) no isolated photons,† (5) one track well-identified as a muon in the muon-counter, with calorimeter energy $< 500\,\text{MeV}$, and the other track well-identified as an electron

⋆ Acoplanarity, θ_{acop}, is defined as the angle between the planes spanned by the beam direction and the momentum vector of e and μ, respectively. Acollinearity, θ_{acol}, is defined as the angle between the momentum vectors of e and μ.

† An isolated photon is defined to have an energy $> 60\,\text{MeV}$ and to be separated from the nearest charged track by $> 12°$.

using a combination of calorimeter, dE/dx and time-of-flight information. Figure 3 shows one of the selected events.

Monte Carlo simulations yield a detection efficiency of $\sim 14\%$ for these selection criteria, independent of energy in the threshold region. The background is estimated by applying the same requirements to five million events from a data sample taken at the J/ψ energy; seven events meet these criteria, corresponding to a background of 0.12 events in the entire $\tau^+\tau^-$ sample.

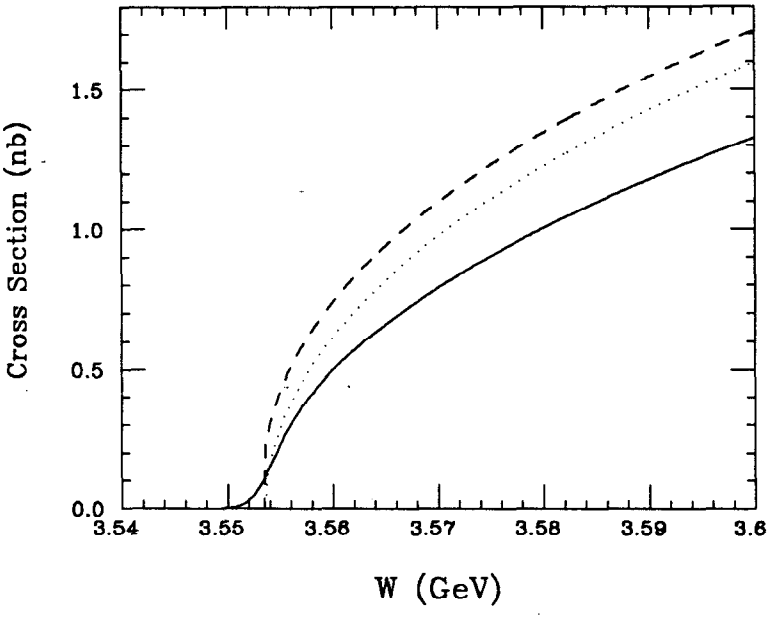

Figure 4. The lowest order Born cross section for $e^+e^- \rightarrow \tau^+\tau^-$ with $m_\tau = 1776.9\,\mathrm{MeV}$ as a function of center-of-mass energy (Equation (2.3), dotted line); after corrections for Coulomb interaction, final state radiation and vacuum polarization (Equation (2.2), dashed line); also including initial state radiation and center-of-mass energy spread (Equation (2.1), full line).

The likelihood function used to estimate the τ mass incorporates the $\tau^+\tau^-$ cross section near threshold (see Figure 4). Including the center-of-mass energy spread Δ, initial state radiation $F(x, W)$,[8] and vacuum polarization corrections

$\Pi(W)$,[9] the cross section is

$$\sigma(W, m_\tau) = \frac{1}{\sqrt{2\pi}\Delta} \int_0^\infty dW' e^{\frac{-(W-W')^2}{2\Delta^2}} \int_0^{1-\frac{4m_\tau^2}{W'^2}} dx F(x, W') \sigma_1(W'\sqrt{1-x}, m_\tau) \ , \quad (2.1)$$

where σ_1 is

$$\sigma_1(W, m_\tau) = \sigma_0(W, m_\tau) \frac{F_c(\beta) F_r(\beta)}{[1 - \Pi(W)]^2} \ . \quad (2.2)$$

W is the center-of-mass energy, and $\beta = \sqrt{1 - \left(\frac{2m_\tau}{W}\right)^2}$. The Coulomb interaction and final state radiation corrections are described by the functions $F_c(\beta)$ and $F_r(\beta)$.[10] The lowest order Born cross section, σ_0, is given by

$$\sigma_0(W, m_\tau) = \frac{4\pi\alpha^2}{3W^2} \frac{\beta(3-\beta^2)}{2} \quad (2.3)$$

The likelihood function is a product of Poisson distributions, one for each center-of-mass energy at which data were taken during a scan of the $\tau^+\tau^-$ threshold region. At each point, the number of expected $e - \mu$ events $\langle N \rangle$, is given by:

$$\langle N \rangle = [\epsilon \ B \ \sigma(W, m_\tau) + \sigma_B] \mathcal{L}. \quad (2.4)$$

Here ϵ is the detection efficiency, B is the product branching fraction for $\tau^+\tau^-$ decay to $e - \mu$, $\mathcal{L}$ is the integrated luminosity at the point in question. and σ_B is the effective background cross section estimated from the J/ψ data sample ($\sigma_B = 0.024\,\text{pb}$).

Since the range of center-of-mass energies where the $\tau^+\tau^-$cross section is most sensitive to the τ mass is of the order of the beam energy spread around $\tau^+\tau^-$ threshold, it is important to devise a running strategy to maximize the integrated luminosity in this region. The beam energy is set initially assuming the world average for the τ mass, in this case the Particle-Data-Group (PDG) value

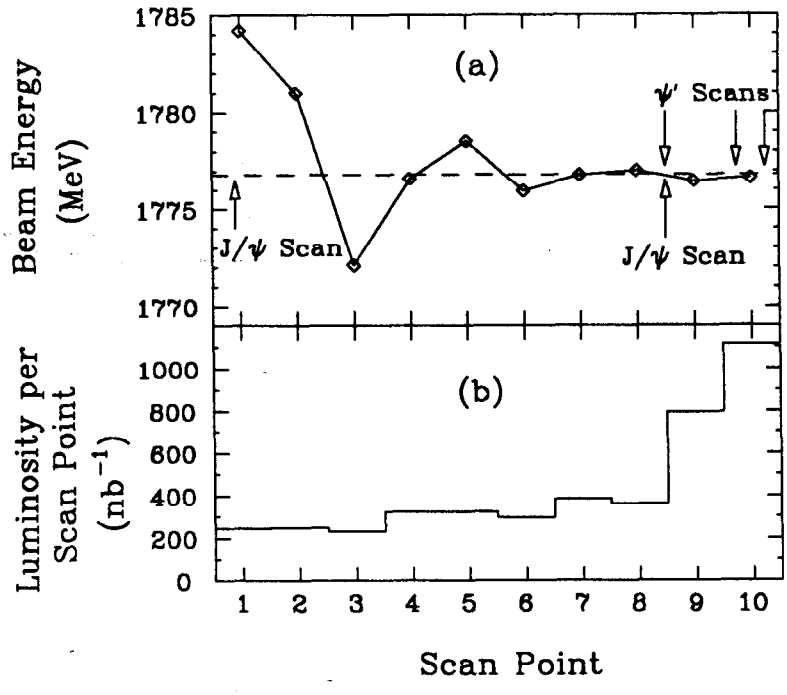

Figure 5. (a) The convergence of the predicted τ mass with each consecutive scan point. (b) The integrated luminosity at each point.

of 1784.1 MeV. Then, after each $250 - 400\,\mathrm{nb}^{-1}$ of integrated luminosity, a new estimate of the mass is made using all the data accumulated to that point; in this way a new prediction of the most sensitive center-of-mass energy at which to run is obtained. The energy is changed to this new value if the difference is more than the BEPC step size (~ 0.4 MeV). Following this strategy, an integrated luminosity of about $4.3\,\mathrm{pb}^{-1}$ has been accumulated at ten energies within a W-range of 24 MeV. It has been verified by Monte Carlo simulation that this data-driven search strategy provides an unbiased measurement.

The sequence of beam energies is shown in Figure 5; the corresponding data are summarized in Table 1. The ten-step search yielded seven $e - \mu$ events. The eleventh and twelfth points in Table 1, taken well above threshold where the cross section varies slowly with energy, provide an improved estimate of the absolute $\tau^+\tau^-$ cross section.

Table 1. A chronological summary of the $\tau^+\tau^-$ data.

Scan Point	$W/2$ (MeV)	$\Delta^\dagger$ (MeV)	$\mathcal{L}$ (nb^{-1})	N ($e-\mu$ events)
1	1784.19	1.34	245.8	2
2	1780.99	1.33	248.9	1
3	1772.09	1.36	232.8	0
4	1776.57	1.37	323.0	0
5	1778.49	1.44	322.5	2
6	1775.95	1.43	296.9	0
7	1776.75	1.47	384.0	0
8	1776.98	1.47	360.8	1
9	1776.45	1.44	794.1	0
10	1776.62	1.40	1109.1	1
11	1799.51	1.44	499.7	5
12	1789.55	1.43	250.0	2

In order to account for uncertainties in the efficiency ϵ, the branching fraction product and the luminosity, ϵ is treated as a free parameter in a two-dimensional maximum-likelihood fit for m_τ and ϵ to the data of Table 1. The results obtained are $m_\tau = 1776.9\,\mathrm{MeV}$ and $\epsilon = 14.1\%$. The uncertainty in ϵ is equivalent to the uncertainty in the absolute normalization, and is treated as a source of systematic error. The statistical error in m_τ, $^{+0.4}_{-0.5}\,\mathrm{MeV}$,* is determined from the one-parameter likelihood function with ϵ fixed to 14.1% (Figure 6(c)). The efficiency-corrected cross section data as a function of center-of-mass energy and the curve which results from the likelihood fit are shown in Figure 6. The quality of the fit is checked by

† Δ was determined according to the equation $\Delta = (A\bar{I} + B)(CW^2 + D)$, where $\bar{I}$ is the average beam current. A, B, C and D are fitted to beam current measurements and to measurements of the energy spreads at the J/ψ and ψ' resonances.

⋆ It has been verified by simulation that this uncertainty corresponds to a 68% confidence interval.

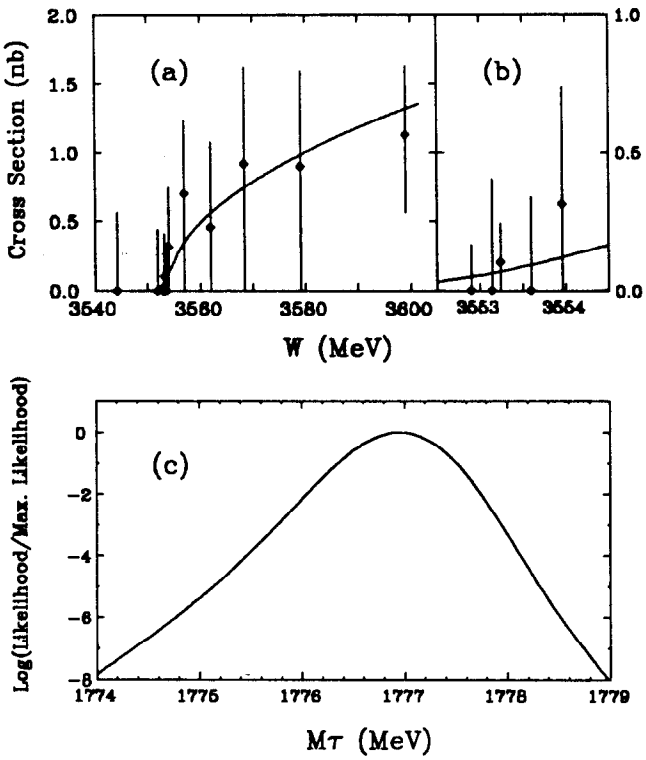

Figure 6. (a) The center-of-mass energy dependence of the $\tau^+\tau^-$ cross section resulting from the likelihood fit (curve), compared to the efficiency-corrected data. The error bars represent 68% Poissonian confidence intervals. (b) An expanded version of (a), in the immediate vicinity of $\tau^+\tau^-$ threshold. (c) The dependence of the logarithm of the likelihood function on m_τ, with efficiency fixed at 14.1%.

forming the likelihood ratio λ, with result $-2\ln\lambda = 3.6$.†

Four independent sources of systematic error have been considered : uncertainties in the product $\epsilon B\mathcal{L}$, in the absolute beam energy scale, in the beam energy spread, and in the background.

The systematic uncertainty in $\epsilon B\mathcal{L}$ is determined by fixing m_τ at its best-estimate value and finding the values of ϵ corresponding to $\pm 1\sigma$ variations in the likelihood function; these efficiencies are 18.3% and 10.6%. Fixing the efficiency to each of these values in turn and fitting for m_τ yields changes in the predicted

† In the large statistics limit $-2\ln\lambda$ would obey a χ^2 distribution for ten degrees of freedom.

mass of $\Delta m_\tau = {}^{+0.16}_{-0.20}$ MeV.

The energy scale is determined from several scans of the J/ψ and ψ' resonances (see Figure 7). These scans were performed during the search at the points indicated by the arrows in Figure 5. The reproducibility of the fits to the scans, together with the other uncertainties listed in Table 2, yields a systematic uncertainty of $\Delta m_\tau = \pm 0.09$ MeV.*

Table 2. Contributions to the uncertainty in the energy scale.

Quantity	Error (MeV)
W_M : BEPC measured center-of-mass energy	$\delta W_M = 0.10$
$M_\psi = 3097.20$ MeV : BEPC value for J/ψ mass	$\delta M_\psi = 0.18$
$M_{\psi'} = 3686.88$ MeV : BEPC value for ψ' mass	$\delta M_{\psi'} = 0.15$
T_ψ : PDG value for J/ψ mass[5]	$\delta T_\psi = 0.09$
$T_{\psi'}$: PDG value for ψ' mass[5]	$\delta T_{\psi'} = 0.10$

Fits to the two resonances were also used to measure the beam energy spread and its variation with center-of-mass energy and beam current. The uncertainty in center-of-mass energy spread is ± 0.08 MeV, yielding a systematic error $\Delta m_\tau = \pm 0.02$ MeV.

The final source of systematic error, uncertainty in the background, is estimated from the 1σ Poisson errors on the seven J/ψ background events and the uncertainty in the hadronic cross section at $\tau^+\tau^-$ threshold. The resulting uncertainty is $\Delta m_\tau = \pm 0.01$ MeV.

These independent systematic errors are added in quadrature to yield a total systematic error of $\Delta m_\tau = {}^{+0.18}_{-0.22}$ MeV.

---

* Assuming a linear relation between measured energy W_M, and the corrected value W, the latter is given by :

$$W = T_\psi + (W_M - M_\psi)\left(\frac{T_{\psi'} - T_\psi}{M_{\psi'} - M_\psi}\right)$$

in the notation of Table 2. At $\tau^+\tau^-$ threshold the resulting mass scale correction is $W - W_M = -0.74$ MeV, with corresponding uncertainty $\delta W = 0.18$ MeV.

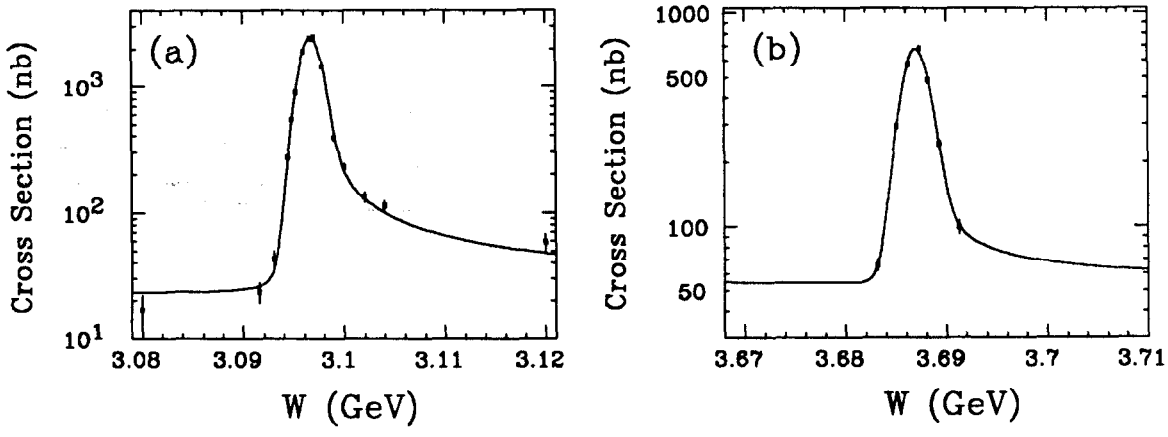

Figure 7. (a) Visible cross section for $e^+e^- \rightarrow$ *hadrons* versus center-of-mass energy in the J/ψ region. (b) Visible cross section for $e^+e^- \rightarrow$ *hadrons* versus center-of-mass energy in the ψ' region.

In conclusion, using a maximum likelihood fit to the $\tau^+\tau^-$ production cross section data near threshold, the BES experiment has measured the mass of the τ lepton as $m_\tau = 1776.9^{+0.4}_{-0.5} \pm 0.2\,\mathrm{MeV}$, where the first error is statistical and the second systematic. This result is 7.2 MeV below the previous world average[5] and has significantly smaller errors.

3. The ARGUS τ Mass Measurement

The ARGUS experiment (see Reference 1 and references therein) has developed a new method to determine the τ mass in hadronic τ decay. They measure the τ pseudomass distribution in the decay $\tau^- \rightarrow \nu_\tau \pi^- \pi^+ \pi^-$. The τ pseudomass is derived from the measured invariant mass, energy and momentum of the 3π system, together with the beam energy.

The analysis uses a data sample of $341\,\mathrm{pb}^{-1}$, containing about 325,000 produced τ pairs, collected at center-of-mass energies between 9.4 and 10.6 GeV. τ pair events are selected in the 1–versus–3 topology with three identified pions and no

photons on one side (3-prong), and e, μ, π or K and up to four photons on the other side (1-prong). About 11,000 events pass the selection criteria with an estimated τ pair background of about 20%. The dominant fraction of this background is from $\tau^- \to \nu_\tau \pi^- \pi^+ \pi^- \pi^\circ$, where the photons from the π° escape detection. There are further background contributions of about 3%, 1% and 1% from multihadrons, radiative bhabhas and two-photon processes, respectively.

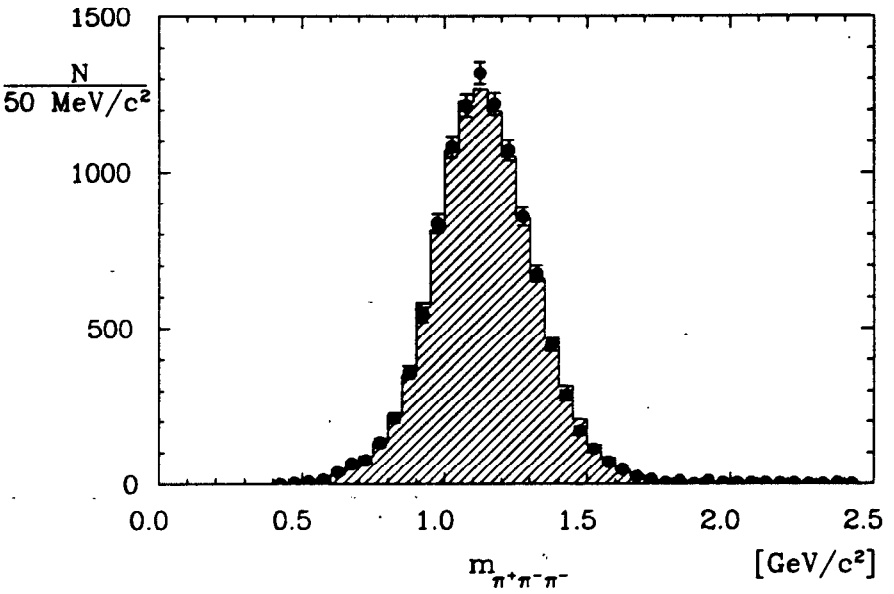

Figure 8. Measured 3π invariant mass spectrum (error bars). The hatched histogram shows the Monte Carlo expectation for signal plus background contributions (see text), normalized to the data.

The measured 3π invariant mass spectrum is shown in Figure 8 together with the Monte Carlo expectation for $\tau^- \to \nu_\tau \pi^- \pi^+ \pi^-$ plus the above mentioned background sources. There is good agreement between data and Monte Carlo. Note that the small number of entries above the τ mass demonstrate that the non-τ background is very small indeed.

A τ pseudomass, m_τ^*, in hadronic τ decay, $\tau \to \nu_\tau + hadrons$, can be derived

in the following way:

$$\underline{p}_\tau = \underline{p}_\nu + \underline{p}_h \ .$$

$$\begin{aligned} m_\tau^2 &= m_\nu^2 + m_h^2 + 2\underline{p}_\nu \underline{p}_h \\ &= m_\nu^2 + m_h^2 + 2(E_\nu E_h - \vec{p}_\nu \vec{p}_h) \\ &= m_\nu^2 + m_h^2 + 2E_\nu E_h - 2|\vec{p}_\nu||\vec{p}_h|\cos(\nu, h) \ . \end{aligned}$$

With $E_\nu = E_\tau - E_h$ and $|\vec{p}_\nu| = \sqrt{E_\nu^2 - m_\nu^2} = \sqrt{(E_\tau - E_h)^2 - m_\nu^2}$,

$$m_\tau^2 = m_\nu^2 + m_h^2 + 2E_\tau E_h - 2E_h^2 - 2|\vec{p}_h|\sqrt{(E_\tau - E_h)^2 - m_\nu^2}\cos(\nu, h) \ .$$

Setting $m_\nu = 0$ and $\cos(\nu, h) = 1$,

$$\begin{aligned} m_\tau^{*\,2} &= m_h^2 + 2E_\tau E_h - 2E_h^2 - 2|\vec{p}_h|(E_\tau - E_h) \\ &= m_h^2 + 2(E_\tau - E_h)(E_h - |\vec{p}_h|) \\ &= m_h^2 + 2(E_{beam} - E_h)(E_h - |\vec{p}_h|) \ , \quad \text{where} \quad E_\tau = E_{beam} \ . \end{aligned} \tag{3.1}$$

The observed τ pseudomass spectrum is shown in Figure 9 together with the Monte Carlo expectation for the above mentioned background sources. The data exhibit a sharp threshold behavior in the region close to the nominal value of the τ mass, while the background is rather smooth in that region. The tail above the nominal τ mass is due to initial-state radiation lowering the τ energy below the beam energy, which leads to an overestimated value for the τ pseudomass. The position of the pseudomass threshold is directly related to the the true mass of the τ lepton.

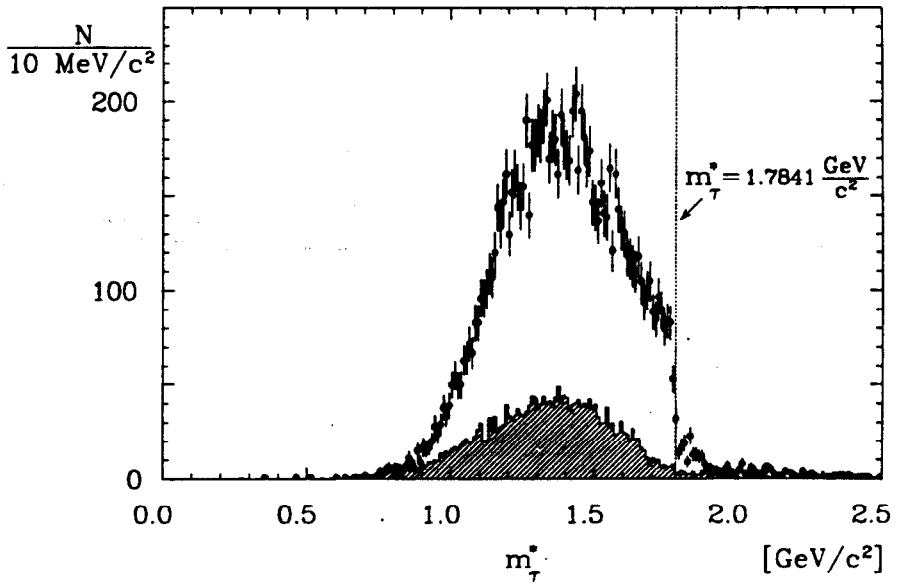

Figure 9. τ pseudomass spectrum for data (error bars) and normalized background (hatched histogram). The PDG τ mass value of 1784.1 MeV is indicated by the dotted line.

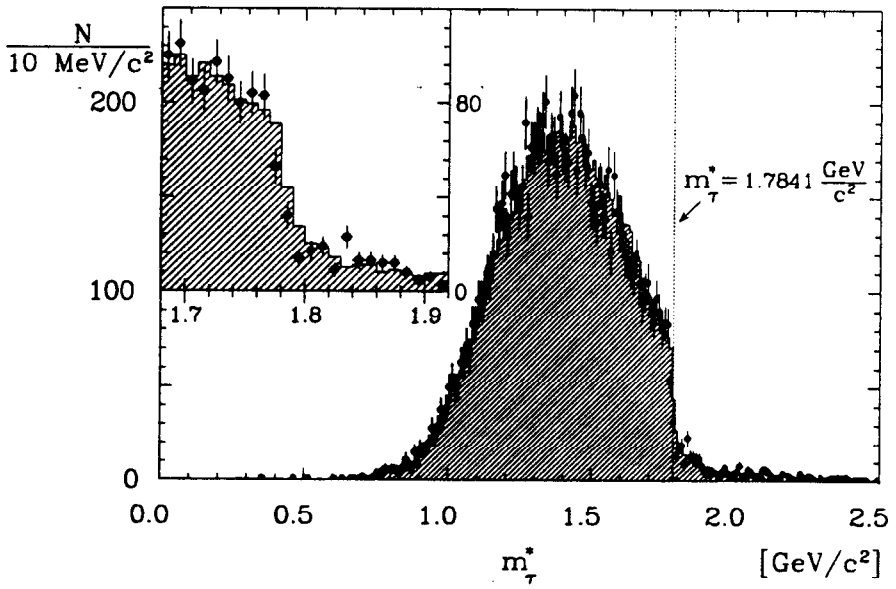

Figure 10. Measured τ pseudomass spectrum (error bars), and Monte Carlo expectation for signal plus background normalized to the data (hatched histogram). The PDG τ mass value of 1784.1 MeV is indicated by the dotted line. The inset shows an enlarged view of the region around that value.

In Figure 10, the measured pseudomass spectrum is compared to the Monte Carlo expectation for signal plus background contributions, simulated with a nominal τ mass of $m_\tau = 1784.1\,\mathrm{MeV}$. While the high-pseudomass tail is well reproduced by the Monte Carlo, the threshold in the data is shifted downward from the Monte Carlo threshold, indicating that the τ mass is smaller than the nominal value used in the simulation.

Monte Carlo studies show that a shift δm_τ in the simulated τ mass results in that same shift in the position of the threshold in the pseudomass spectrum, provided δm_τ is small. The threshold position in the data is determined from a fit with parametrized functions for signal and background contributions obtained from the Monte Carlo, leaving only m_τ and the individual normalizations as free parameters. The result is $m_\tau = 1776.3 \pm 2.4\,\mathrm{MeV}$, where only the statistical error is given. Figure 11 shows the measured pseudomass spectrum together with the fitted functions. The threshold behavior and the background level are well reproduced by the fit.

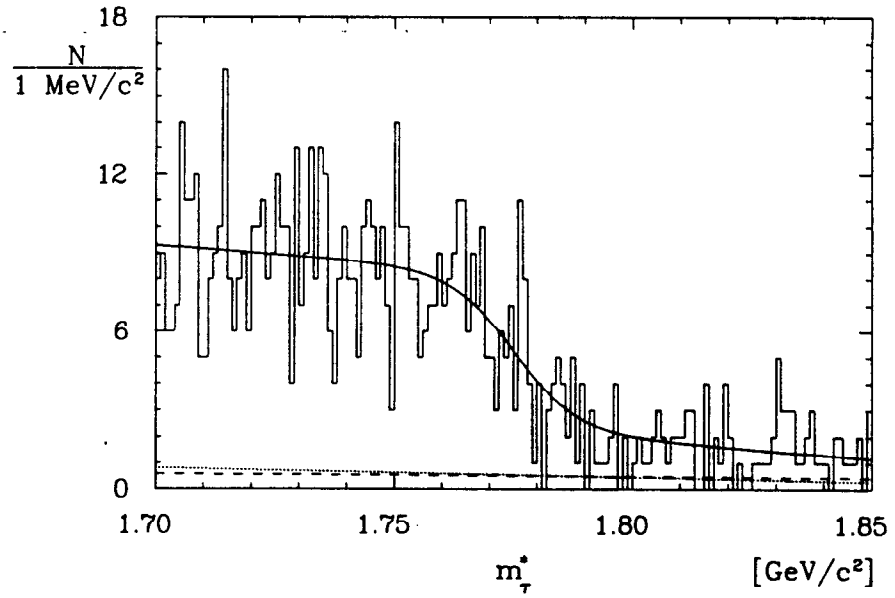

Figure 11. Measured τ pseudomass spectrum in the region of the PDG τ mass value of 1784.1 MeV. The solid curve shows the result of the fit described in the text (dashed line: fitted background, dotted line: expected background).

Various sources of systematic error have been investigated (see Table 3). Adding all contributions in quadrature gives a total systematic error on the τ mass of $\pm 1.4\,\mathrm{MeV}$.

Table 3. Systematic error contributions for the ARGUS τ mass measurement.

Source of error	Uncertainty	m_τ uncertainty
Absolute momentum scale	$\pm 0.15\%$	$\pm 1.2\,MeV$
Beam energy	$\pm 3\,MeV$	$\pm 0.5\,MeV$
Fit region		
Background contributions		$\pm 0.5\,MeV$
MC parametrization		
Signal shape		
Total		$\pm 1.4\,MeV$
Non-zero τ neutrino mass	$m(\nu_\tau) = 20\,MeV$	$+0.3\,MeV$

In conclusion, investigating the τ pseudomass spectrum in decays of the type $\tau^- \rightarrow \nu_\tau \pi^- \pi^+ \pi^-$, the ARGUS experiment has measured the mass of the τ lepton as $m_\tau = 1776.3 \pm 2.4 \pm 1.4\,\mathrm{MeV}$, where the first error is statistical and the second systematic.

4. The CLEO τ Mass Measurement

The CLEO experiment (see Reference 3 and references therein) has developed yet another method to determine the τ mass in hadronic τ decay. They analyze the distribution of the minimum kinematically allowed τ mass in hadronic τ decay, $\tau \rightarrow \nu_\tau + hadrons$. The minimum kinematically allowed τ mass is determined from the measured energies and momenta of the hadronic system, together with the beam energy.

The analysis uses a data sample of $1430\,\mathrm{pb}^{-1}$, containing about 1,310,000 produced τ pairs, collected at center-of-mass energies around 10.6 GeV. τ pair events

are selected in the 1–versus–1 topology where each τ decays hadronically into one charged particle (assumed to be a π) and up to two π^0's; there has to be at least one π^0 in an event. About 28,000 events pass the selection criteria with an estimated background from multihadrons, QED and two-photon processes of less than 1% total.

In a hadronic two-body decay, $\tau \rightarrow \nu_\tau + hadrons$, the τ direction lies on a cone of half-angle θ around the direction of the hadronic system:*

$$\underline{p}_\nu = \underline{p}_\tau - \underline{p}_h \ .$$

$$\begin{aligned} m_\nu^2 &= m_\tau^2 + m_h^2 - 2\underline{p}_\tau \underline{p}_h \\ &= m_\tau^2 + m_h^2 - 2(E_\tau E_h - \vec{p}_\tau \vec{p}_h) \\ &= m_\tau^2 + m_h^2 - 2E_\tau E_h + 2|\vec{p}_\tau||\vec{p}_h|\cos(\tau, h) \ . \end{aligned}$$

Setting $E_\tau = E_{beam}$ and $|\vec{p}_\tau| = \sqrt{E_{beam}^2 - m_\tau^2}$,

$$\cos\theta(1) = \frac{m_\nu^2 - m_\tau^2 - m_{h(1)}^2 + 2E_{beam}E_{h(1)}}{2\sqrt{E_{beam}^2 - m_\tau^2}\ |\vec{p}_{h(1)}|} \qquad (4.1)$$

$$\cos\theta(2) = \frac{m_\nu^2 - m_\tau^2 - m_{h(2)}^2 + 2E_{beam}E_{h(2)}}{2\sqrt{E_{beam}^2 - m_\tau^2}\ |\vec{p}_{h(2)}|} \ .$$

In the absence of initial state radiation, both τ's in the event have the beam energy and are back-to-back. Thus, the true τ direction must lie on the intersection of one cone and the parity-inversion of the other cone (see Figure 12(a)). In general, two cones intersect in two rays. If one assumes a smaller τ mass the two half-angles shrink; eventually, the two cones just touch. Since further shrinking of the τ mass yields τ directions which cannot be back-to-back, this degenerate solution is the

* At CESR energies, θ is typically around 8°.

so-called minimum kinematically allowed τ mass for the event, M_{min}. At this point, the directions of both τ's and both hadronic systems lie in a plane and one has $\theta_1 + \theta_2 + \phi = \pi$, where ϕ is the angle between the two hadronic systems (see Figure 12(b)). With this relation, the above equations can be solved for the value of M_{min} for that event.

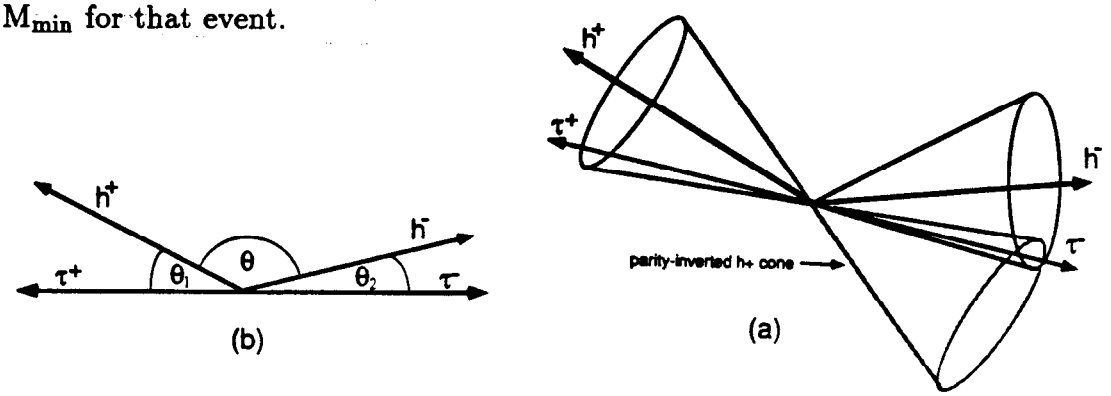

Figure 12. (a) The kinematics in hadronic τ decay of two back-to-back τ's. (b) The degenerate case for the minimum kinematically allowed τ mass.

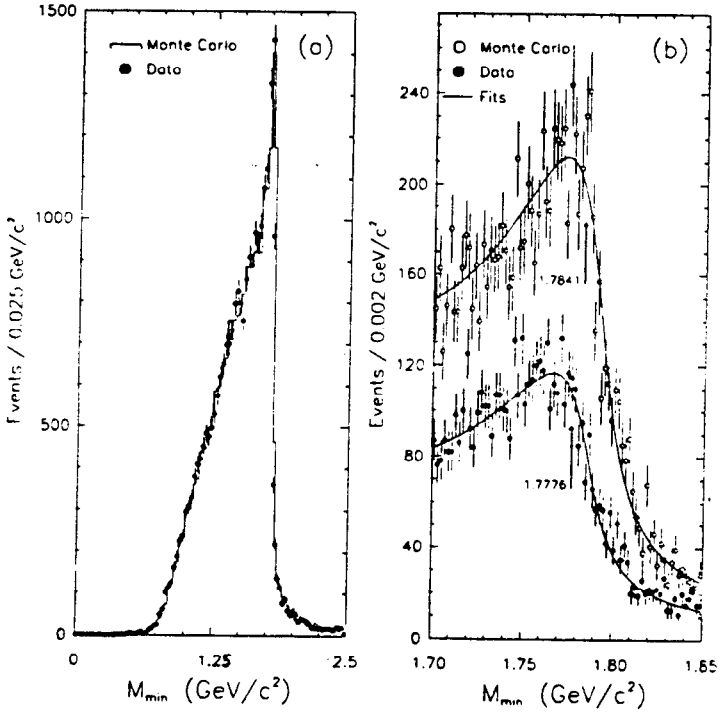

Figure 13. (a) The M_{min} distribution in data (error bars) and Monte Carlo (histogram). (b) An expanded view of (a) in the region around the PDG τ mass value for data (full circles with error bars) and Monte Carlo (empty circles with error bars, arbitrary vertical scale). Superimposed (solid lines) are the fit results (see text).

Figure 13(a) shows the M_{min} distribution in the data. It exhibits a pileup of events just below the τ mass, followed by a sharp drop and a small high-mass tail. These features are well reproduced by a Monte Carlo simulation of the signal,* including initial state radiation, beam energy spread, missed and misidentified particles and finite detector resolution. The simulation shows that the position of the edge in the M_{min} distribution linearly tracks the true τ mass; a shift in m_τ results in a corresponding shift in the edge in M_{min}.

The data are fit with a parametrized function obtained from the Monte Carlo, leaving only the position of the edge and the overall normalization as free parameters. The fits, shown as curves superimposed on Figure 13(b) in the region around the τ mass, yield $m_\tau = 1777.6 \pm 0.9\,\mathrm{MeV}$, where the error is statistical only.

Various sources of systematic error have been investigated (see Table 4). Adding all contributions in quadrature gives a total systematic error on the τ mass of $\pm 1.5\,\mathrm{MeV}$.

Table 4. Systematic error contributions for the CLEO τ mass measurement.

Source of error	Scale uncertainty	m_τ uncertainty
Calorimeter energy scale	$\pm 0.3\%$	$\pm 1.2\,MeV$
Momentum scale	$\pm 0.1\%$	$\pm 0.8\,MeV$
Beam energy scale	$\pm 0.03\%$	$\pm 0.1\,MeV$
Cuts, fitting procedure	-	$\pm 0.5\,MeV$
Total		$\pm 1.5\,MeV$
Tau neutrino mass	$< 35\,MeV$ @ 95% C.L.	$+0.9\,MeV$

In conclusion, investigating the minimum kinematically allowed τ mass in hadronic τ decay, the CLEO experiment has measured the mass of the τ lepton as $m_\tau = 1777.6 \pm 0.9 \pm 1.5\,\mathrm{MeV}$, where the first error is statistical and the second systematic.

$\star$ It has been verified that none of the backgrounds produces a structure in the M_{min} distribution in the region of interest.

5. Conclusions

We have presented three new measurements of the mass of the τ lepton. The BES experiment, operating at center-of-mass energies in the $\tau^+\tau^-$ threshold region, measures the τ mass from the energy dependence of the τ pair *production* cross section. In contrast, the ARGUS and CLEO experiments, operating at center-of-mass energies around 10 GeV, get the τ mass using novel methods analyzing the kinematics in hadronic τ *decay*.

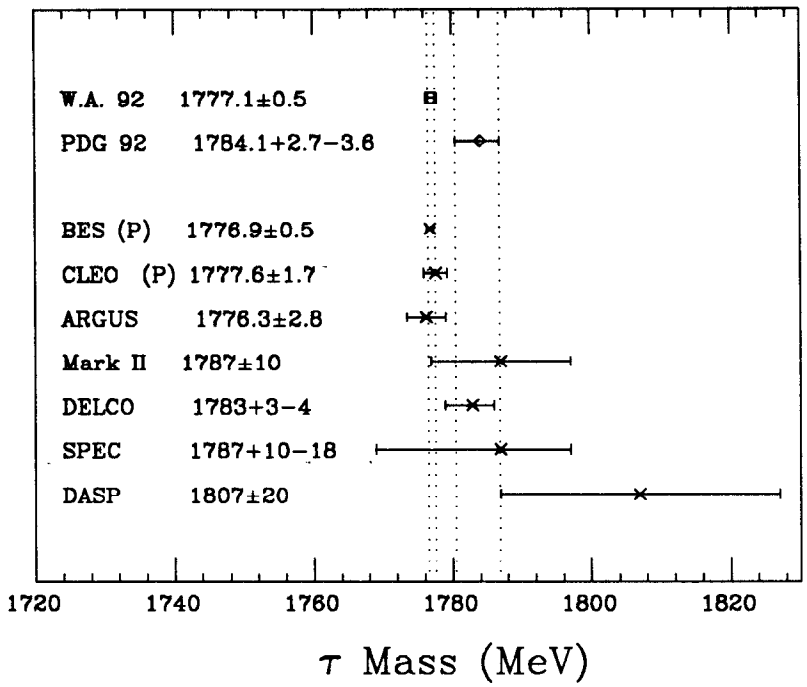

Figure 14. Existing τ mass measurements; (P) indicates a preliminary result. Also shown are the new and old world average (W.A. 92 and PDG 92, respectively).

All three measurements are in excellent agreement despite the very different systematics and have much improved precision. They yield a new world average of

$$m_\tau = 1777.1 \pm 0.5\,\text{MeV}\ , \tag{5.1}$$

which is 7 MeV and about 2 standard deviations below the previous value (see Figure 14).

Inserting this new τ mass value and an updated τ lifetime,[11] $\tau_\tau = 295.7 \pm 3.2$ fs, and electronic branching fraction, $B_e = 17.76 \pm 0.15\%$, into Equation (1.1), the coupling strength ratio becomes†

$$\frac{G_F^2(\tau)}{G_F^2(\mu)} = 0.980 \pm 0.011 \pm 0.008 \pm 0.001 \ . \tag{5.2}$$

Note that the deviation from lepton universality, *i.e.*, $\frac{G_F^2(\tau)}{G_F^2(\mu)} = 1$, is reduced from 2.4 to only 1.4 standard deviations, due to significant decreases in τ lifetime as well as τ mass; this is illustrated in Figure 15.

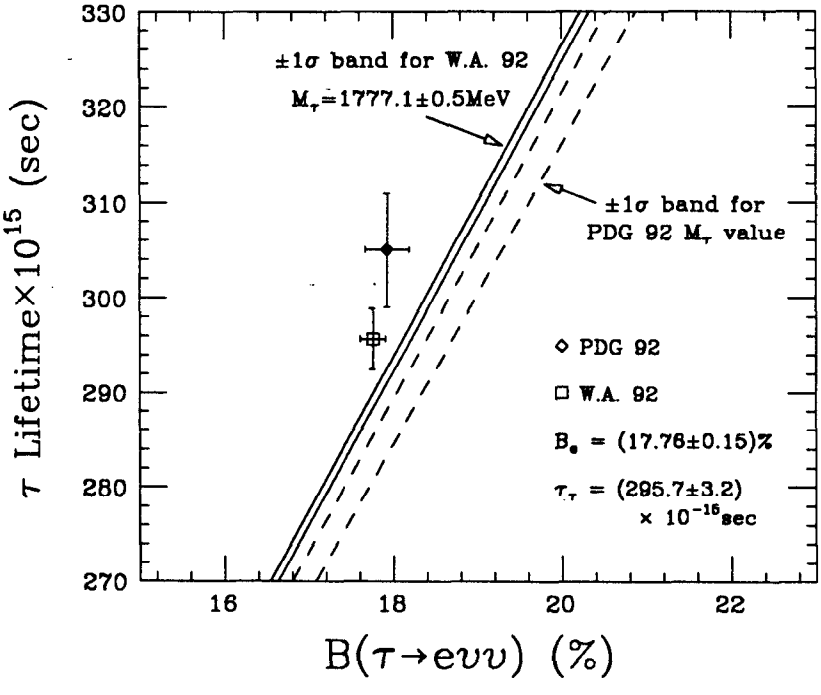

Figure 15. The variation of τ_τ with B_e, given by Equation (1.1) under the assumption of lepton universality, in comparison to the points representing the new and old world averages (W.A. 92 and PDG 92, respectively) of the direct measurements.

† Again, the error contributions from the lifetime, the electronic branching fraction and the mass are listed separately. Note that the error contribution from the mass has become almost negligible.

It has thus become questionable whether there still exists a consistency problem. Certainly, due to its increased precision, the τ mass cannot be the source of any remaining discrepancy.

ACKNOWLEDGEMENTS

The author would like to thank members of the ARGUS, BES and CLEO experiments for helpful discussions in preparing this presentation. In addition, the author thanks all those involved in the organization of this workshop.

REFERENCES

1. H. Albrecht *et al.*, *Phys. Lett.* **B292** (1992), 221.
2. J. Z. Bai *et al.*, SLAC–PUB–5870, July 1992; submitted to *Phys. Rev. Lett.*
3. *M. Daoudi et al., Proceedings of the XXVI International Conference on High Energy Physics*, Dallas (1992).
4. W. J. Marciano and A. Sirlin, *Phys. Rev. Lett.* **61** (1988), 1815.
5. K. Hikasa *et al.*, Review of Physical Properties, *Phys. Rev.* **D45** (1992), Part II.
6. W. Bacino *et al.*, *Phys. Rev. Lett.* **41** (1978), 13.
7. M. H. Ye and Z. P. Zheng, *Proceedings of the 1989 International Symposium on Lepton and Photon Interactions at High Energies*, Stanford (1989).
8. É. A. Kuraev and V. S. Fadin, *Yad. Fiz.* **41** (1985), 733.
9. F. A. Berends and G. J. Komen, *Phys. Lett.* **63B** (1976), 432.
10. M. B. Voloshin, Preprint TPI–MINN–89–33–T, Nov. 1989.
11. W. Trischuk, invited talk at this workshop.